Neuroscience

The Journal of Physiology

JPn

Neuronal detection thresholds during vestibular compensation: contributions of response variability and sensory substitution

Mohsen Jamali[1], Diana E. Mitchell[1], Alexis Dale[1], Jerome Carriot[1], Soroush G. Sadeghi[1,2] and Kathleen E. Cullen[1]

[1]*Department of Physiology, McGill University, Montreal, Quebec H3G 1Y6, Canada*
[2]*Department of Cummunicative Disorders and Sciences, University at Buffalo, The State University of New York, Buffalo, NY 14214, United States*

Key points

- Unilateral vestibular injury impairs our ability to detect motion. However, before this study the neural mechanisms underlying this impairment had not yet been established.
- We found that the detection thresholds of neurons at the first central stage of vestibular processing (i.e. vestibular nuclei) dramatically increase immediately post-lesion, and despite some recovery remain elevated even after 1 month, following the trend reported for vestibular patients' perception.
- After the lesion, parallel changes in neuronal trial-to-trial variability and sensitivity account for consistently elevated thresholds, thus providing a neural correlate for impaired behavioural performance.
- In a subset of neurons, sensory substitution with extravestibular (i.e. proprioceptive) inputs after the lesion combined with residual vestibular information serves to improve neuronal detection thresholds for head-on-body motion.
- Our results provide a neural correlate for rehabilitation approaches that take advantage of the convergence of proprioceptive and vestibular inputs to improve patient outcomes.

Abstract The vestibular system is responsible for processing self-motion, allowing normal subjects to discriminate the direction of rotational movements as slow as 1–2 deg s^{-1}. After unilateral vestibular injury patients' direction–discrimination thresholds worsen to $\sim$20 deg s^{-1}, and despite some improvement thresholds remain substantially elevated following compensation. To date, however, the underlying neural mechanisms of this recovery have not been addressed. Here, we recorded from first-order central neurons in the macaque monkey that provide vestibular information to higher brain areas for self-motion perception. Immediately following unilateral labyrinthectomy, neuronal detection thresholds increased by more than two-fold (from 14 to 30 deg s^{-1}). While thresholds showed slight improvement by week 3 (25 deg s^{-1}), they never recovered to control values – a trend mirroring the time course of perceptual thresholds in patients. We further discovered that changes in neuronal response variability paralleled changes in sensitivity for vestibular stimulation during compensation, thereby causing detection thresholds to remain elevated over time. However, we found that in a subset of neurons, the emergence of neck proprioceptive responses combined with residual vestibular modulation during head-on-body motion led to better neuronal detection thresholds. Taken together, our results emphasize that increases in response variability to vestibular inputs ultimately constrain neural thresholds and provide evidence that sensory substitution with extravestibular (i.e. proprioceptive) inputs at the first central stage of vestibular processing is a neural substrate for improvements in self-motion perception following vestibular loss. Thus, our results provide a neural correlate for the patient benefits provided by rehabilitative strategies that take advantage of the convergence of these multisensory cues.

Corresponding author K. Cullen: McGill University, Aerospace Medical Research Unit, MacIntyre Medical Sciences Bldg, 3655 Prom Sir William Osler, Montreal, Quebec, Canada, H3G 1Y6.   Email: kathleen.cullen@mcgill.ca

Abbreviations   ISI, interspike interval; VAF, variance accounted for; VO, vestibular-only; VOR, vestibulo-ocular reflex.

Introduction

The vestibular system is essential for encoding head movement-related information required for our perception of self-motion, as well as for the generation of reflexes to ensure for ensuring postural and gaze stability. Normal subjects can discriminate the direction (i.e. leftward or rightward) of horizontal rotational movements as slow as 1 or 2 deg s^{-1} (Seemungal *et al.* 2004; Grabherr *et al.* 2008; Mallery *et al.* 2010). In contrast, patients with complete loss of vestibular function exhibit significantly increased direction–discrimination thresholds (e.g. 5–15 times higher; Valko *et al.* 2012). Thus, vestibular sensory information makes a vital contribution to the perception of self-motion.

Early vestibular pathways can show remarkable plasticity in response to the effects of ageing, disease and peripheral trauma. Previous studies have largely focused on compensation in the pathways that mediate the vestibulo-ocular reflex (VOR) after unilateral vestibular loss. Notably, there is a strong relationship between the recovery of motor performance after lesion and the recovery of vestibular sensitivity in single neurons constituting the first central stage of processing (anaesthetized preparations: reviewed by Straka *et al.* 2005; alert rhesus monkeys: Sadeghi *et al.* 2010). Compensation is also characterized by sensory substitution with other self-motion inputs (i.e. proprioceptive and motor related) at the level of these same central vestibular neurons (Sadeghi *et al.* 2010). A recent study similarly demonstrated dynamic reweighting of vestibular and extravestibular inputs within vestibulospinal pathways (Sadeghi *et al.* 2011) that likewise parallels behavioural recovery (i.e. postural reflexes; reviewed in Smith & Curthoys, 1989) after vestibular lesion. To date, however, the neural mechanisms by which the perception of self-motion recovers following vestibular loss are not understood.

Rotational direction–discrimination thresholds in patients worsen to ∼20 deg s^{-1} in the first days after unilateral vestibular loss for movements towards the affected side (Cutfield *et al.* 2011), and then show recovery but remain elevated after 1–2 months (Cousins *et al.* 2013). Accordingly, we hypothesized that neuronal detection thresholds for vestibular as well as extravestibular cues may change in parallel with improvements in vestibular perception. To test this, we recorded from the neurons at the first central stage of vestibular processing, which

are thought to be essential for computation of spatial orientation as well as self-motion perception based on their reciprocal interconnections with the cerebellum and projections to the thalamus (reviewed in Cullen, 2012).

We found that, immediately following the lesion, neuronal detection thresholds substantially increased and never fully recovered. Notably, the time course and extent of improvement were comparable to those reported for rotational direction–discrimination thresholds in patients following unilateral vestibular loss (Cutfield *et al.* 2011; Cousins *et al.* 2013), thereby providing a neural correlate for the observed impaired behavioural performance. Further analysis revealed that, while vestibular sensitivities increased to normal levels within the first month, this modulation increase was accompanied by a corresponding increase in response variability, resulting in a sustained increment in neuronal detection thresholds. Strikingly, however, we also discovered that in a subset of neurons, extravestibular proprioceptive signals, which are up-weighted during compensation (Sadeghi *et al.* 2010, 2011), act synergistically with the vestibular input to bolster the detection of head rotations on the body. Thus, taken together, our results show that (1) the mechanism underlying compensation is constrained by parallel changes in neuronal response sensitivity and variability, and (2) sensory substitution with extravestibular input can potentially lead to beneficial and enduring changes in self-motion processing. These findings support the proposal that rehabilitation approaches that engage this multimodal convergence are probably most effective in improving functional recovery.

Methods

Subjects and surgical preparation

All procedures were approved by both the McGill University Animal Care Committee and the Johns Hopkins University Animal Care and Use Committee, and were in accordance with Canadian Council on Animal Care and National Institutes of Health guidelines. Two rhesus monkeys (*Macaca mulatta*) were each implanted with a stainless steel post for head immobilization, a stainless steel recording chamber for access to the vestibular nuclei, and an eye coil. Surgical techniques and procedures were similar to those described in our previous study (Sadeghi *et al.* 2007*b*). Preoperatively and every 2.5–3 h during surgery, animals were injected

with the anticholinergic glycopyrrolate (0.005 mg kg^{-1} I.M.) to stabilize heart rate and to reduce salivation. Animals were then pre-anaesthetized using ketamine hydrochloride (15 mg kg^{-1} I.M.). Finally, buprenorphine (0.01 mg kg^{-1} I.M.) and diazepam (1 mg kg^{-1} I.M.) were injected as an analgesic and as a muscle relaxant, respectively. To reduce swelling and prevent infection, loading doses of dexamethasone (1 mg kg^{-1} I.M.) and cefazolin (50 mg kg^{-1} I.V.) were administered, respectively. Surgical levels of anaesthesia were then achieved using isoflurane gas, maintained at 0.8–1.5%, together with a minimum 3 l min^{-1} (dose adjusted to effect) of 100% oxygen. Heart rate, blood pressure, respiration and body temperature were monitored throughout the procedure.

Following the implant surgery, dexamethasone (0.5 mg kg^{-1} I.M.) administration was continued for 4 days. Animals were also injected with buprenorphine (0.01 mg kg^{-1} I.M.) for postoperative analgesia (every 12 h for 2–5 days, depending on the animal's pain level), and anafen (2 mg kg^{-1} and then 1 mg kg^{-1} on subsequent days) as an anti-inflammatory. In addition, cefazolin (25 mg kg^{-1} I.M.) was injected twice daily for 10 days to prevent infection. Animals were given at least 2 weeks to recuperate from the surgery before any experiments began. Recordings were made following a brief training period in which monkeys were conditioned to fixate visual targets for juice reward.

Additional recordings were performed after unilateral labyrinthectomy (up to 2 months post-lesion), in which the three semicircular canal ampullae, the utricle and saccule, and the distal ends of ampullary nerve branches were removed as described previously (Sadeghi *et al.* 2006). Briefly, under general anaesthesia as described above, a postauricular incision was made and the mastoid bone was removed to expose the horizontal and posterior semicircular canals. The petrous bone was removed further anteriorly and superiorly to visualize the superior canal near its union with the common crus. Each of the semicircular canals then was obliterated with removal of the ampullae. The vestibule was entered, and the utricle and saccule were removed. The internal auditory canal was opened next, and the distal ends of the ampullary nerve branches were removed. The space created by the labyrinthectomy was packed with muscle and fascia and the postauricular incision was closed. Following the procedure, monkeys again received the postoperative analgesia and antibiotic treatments described above.

Experimental design and data acquisition

Monkeys were initially head-restrained and seated on an earth-vertical axis motion turntable, located within a 1 m^3 magnetic field coil (CNC Engineering, Enfield, CT, USA). A visual target (HeNe laser) was projected on to a cylindrical screen located 60 cm away from the monkey's head. Turntable and target velocity were controlled by a QNX-based real-time data acquisition system (REX; Hayes *et al.* 1982). Standard extracellular recording approaches were used to characterize the sensitivities, thresholds and variability of single vestibular nuclei neuron responses to passively applied vestibular and neck stimulation. We specifically focused on a subclass of vestibular nuclei neurons termed vestibular-only (VO) neurons that respond to rotational vestibular stimulation but are insensitive to eye movements (Roy & Cullen, 2001*b*, 2004), as these neurons are thought to be involved in the computation of spatial orientation as well as the regulation of gait and posture (reviewed in Cullen, 2012).

First, to characterize VO neurons, head-restrained monkeys were rotated (0.5 Hz, ±40 deg s^{-1} peak velocity) about the earth-vertical axis to identify neurons responding to passive horizontal whole-body rotation. Next, to confirm each neuron's insensitivity to eye movements, its activity was recorded while the head-restrained monkey made saccadic and smooth pursuit eye movements to track a visual target stepped between horizontal positions (up to ±30 deg) or moved sinusoidally (0.5 Hz, peak velocity ±40 deg s^{-1}), respectively. In addition, neuronal responses were recorded in a third paradigm where the monkey fixated a head-stationary visual target during whole body rotation (VOR cancellation). Neuronal responses were comparable ($P = 0.51$) to those evoked when the VOR was not cancelled further confirming each neuron's insensitivity to eye movements.

Next, to test neuronal thresholds, three stimulation protocols were applied in total darkness: (1) passive whole-body rotations (i.e. vestibular stimulation; 0.5 Hz, ±40 deg s^{-1} peak velocity) were applied using the vestibular turntable as in the initial neuron characterization above; (2) passive body-under-head rotations (i.e. proprioceptive stimulation; 0.5 Hz, ±40 deg s^{-1} and ±80 deg s^{-1}) were applied by rotating the monkey using the turntable while its head was held stationary in space; and (3) passive head-on-body rotations (i.e. combined vestibular and proprioceptive stimulation; 0.5 Hz, ±40 deg s^{-1}) were applied using a torque motor (Kollmorgen, Richmond, ON, Canada) that was attached to the head (Huterer & Cullen, 2002; Sadeghi *et al.* 2006, 2007*a,b*, 2009). All analyses were performed using a minimum of five cycles of rotation.

Data acquisition

Extracellular, single-unit recordings were made with enamel-insulated tungsten microelectrodes (7–10 MΩ impedance; Frederick Haer, Bowdoin, ME, USA), the depths of which were controlled with a hydraulic microdrive (Narishige, East Meadow, NY, USA or Tokyo, Japan). Neurons were first identified in the abducens

nucleus based on their typical discharge pattern during spontaneous eye movements (Robinson, 1970; Cullen *et al.* 1993; Sylvestre & Cullen, 1999). The medial and lateral vestibular nuclei were then located lateral and posterior to abducens. In the present study, we focus on VO neurons that were recorded in the contralesional vestibular nuclei. Consistent with previous characterizations, these neurons respond only to vestibular stimulation and are insensitive to eye movements (Roy & Cullen, 2001*b*, 2004, Sadeghi *et al.* 2011). VO neurons were then further classified as either type I or type II, based on whether they responded to ipsilaterally or contralaterally directed motion, respectively.

Head and gaze position were acquired using the magnetic search coil technique (Fuchs & Robinson, 1966, Judge *et al.* 1980), and turntable velocity was measured by an angular velocity sensor (Watson Industries, Eau Claire, WI, USA). All behavioural signals were low-pass filtered at 250 Hz, and recorded with the measured extracellular potential on DAT tape for later playback. During playback, action potentials were discriminated by a windowing circuit (BAK Electronics, Inc., Sanford, FL, USA) that was manually set to generate a pulse at the rising phase of each spike. All signals were digitally sampled at 1 kHz.

Recordings were collected from each animal before (normal), and then 15–28 h following labyrinthectomy (day 1). Additional recordings were obtained on a weekly basis up to 2 months post-lesion.

Data analysis

Basic characterization

Neuronal spike trains and behavioural data were imported into the Matlab (The MathWorks, Natick, MA, USA) programming environment. Head and gaze position signals were digitally low-pass filtered at 125 Hz with zero phase distortion using a 51st order finite impulse response filter with a Hamming window. Eye position was then computed as the difference between head and gaze position. Eye, head and gaze velocities were obtained by digitally differentiating position signals. Finally, representations of instantaneous firing rate were computed either by (1) convolving a Kaiser window with the spike train (cut-off frequency 0.1 Hz above stimulus frequency; Cherif *et al.* 2008; Jamali *et al.* 2009, 2013), or (2) using the reciprocal of the interspike interval (Yu *et al.* 2012; Jamali *et al.* 2013). For the latter approach, the inverse of the difference between the timestamps of two consecutive spikes was used to represent firing rate at the time point mid-way between the two.

Neuronal responses during all three conditions (i.e. vestibular stimulation, neck proprioceptive stimulation, and combined stimulation) were characterized using a least-squares regression analysis in which firing rate was estimated as:

$$fr = b_i + S_i \times V_i(t - T_i) \qquad (1)$$

where b_i is a bias term, S_i is the neuron's firing rate sensitivity [(spk s^{-1})/(deg s^{-1})], V_i is the stimulation velocity and T_i represents the neuron's optimal phase shift computed relative to angular velocity, for whole-body rotations ($i = 1$), body-under-head rotations ($i = 2$), and head-on-body rotations ($i = 3$). Note that for body-under-head rotations, neurons with sensitivity greater than 0.1 were used to determine neck proprioception detection thresholds (see below). Sensitivity to combined vestibular and proprioceptive stimulation (S_3) during head-on-body rotation was estimated as the response to head-on-body velocity, and compared to the linear summation of the sensitivities to vestibular (S_1) and neck proprioceptive (S_2) stimulation.

For each least-squares regression analysis, the goodness of fit of a given estimate was quantified by computing the variance accounted for: VAF $= 1-[\text{var}(fr-\text{fr})/\text{var}(\text{fr})]$ (Cullen *et al.* 1996), where fr is the estimated firing rate and fr represents the measured firing rate.

Variability

For a given neuron, the rotational stimulus was shifted by the neuron's estimated phase, and instantaneous firing rate was plotted as a function of the shifted stimulus velocity (Fig. 1*A*). We then computed the mean (μ) and standard deviation (σ) of the distribution of firing rates for each rotational velocity in bins of 2 deg s^{-1}.

Unless otherwise noted, reported response variabilities correspond to the standard deviation of a given neuron's firing rate distribution at velocity zero [$\sigma(0)$ in Fig. 1*A*]. Normalized variabilities were scaled according to each neuron's mean firing rate at velocity zero.

Detection thresholds

We calculated the degree of overlap between the firing rate distribution at velocity I with that at velocity 0 as d' from signal detection theory (Green & Swets, 1966):

$$d'(I) = \frac{|\mu(I) - \mu(0)|}{\sqrt{(\sigma^2(I) - \sigma^2(0))/2}} \qquad (2)$$

Because d' was found to vary linearly with the magnitude of rotational velocity, we fit the data with a line and determined each neuron's detection threshold for a given condition as the rotational velocity at which $d' = 1$ (Fig. 1*B*; Snippe & Koenderink, 1992). We emphasize that we use the term 'detection threshold' for our neuronal thresholds as we determined the smallest change in the angular velocity that gives rise to a noticeable change in the firing rate distribution. In contrast, in the two previous

studies that measured perceptual thresholds in vestibular patients (i.e. Cutfield *et al.* 2011; Cousins *et al.* 2013) subjects discriminated whole body leftward from rightward motion. Accordingly, throughout the paper we use the term direction–discrimination threshold (equivalently referred to as the direction–recognition threshold by Chaudhuri *et al.* 2013) for the perceptual thresholds measured in these behavioural studies.

Statistics

Statistical significance was determined using paired or unpaired Student's *t* tests as well as analysis of variance (i.e. one-way ANOVA). If a significant difference between group means was found using ANOVA, a *post hoc* Tukey test was performed to determine which groups differed from each other. Results are reported (and plotted) as means ± S.E.M. and the level of statistical significance was set at $P < 0.05$ unless otherwise stated.

Results

To understand the brain's ability to re-establish network function after vestibular loss requires not only an assessment of the recovery of neuronal response sensitivities but also the determination of whether the observed changes lead to improvements in neural detection thresholds, which are a measure of signal-to-noise. We begin by considering the linkage between changes in neuronal vestibular sensitivities and detection thresholds after unilateral labyrinthectomy for neurons at the first central stage of processing. Note that, while sensitivity simply measures the depth of a neuron's response to a given stimulus, threshold measurements take into account both a neuron's responsiveness and the variability of its response. We then determine whether changes in response variability and sensitivity constrain improvements in the ability of neurons to discriminate between stimuli. Finally, we address whether the extravestibular responses present following vestibular loss (but not before lesion) improve neural detection thresholds.

Vestibular detection thresholds

We directly measured the signals encoded at the first central stage of vestibular processing (the vestibular nuclei). Specifically, we recorded single-unit responses from individual VO neurons, which receive a strong monosynaptic drive from the ipsilateral VIII nerve and, in turn, project to the spinal cord (Wilson *et al.* 1990; Boyle, 1993; Boyle *et al.* 1996; Gdowski & McCrea, 1999) as well as to higher centres such as the thalamus and cortex (Meng *et al.* 2007; Marlinski & McCrea, 2008*a*,*b*). These neurons can be easily identified by their characteristic responses:

increase in firing rate during ipsilaterally directed (type I, $n = 91$) or contralaterally directed (type II, $n = 88$) head rotations, and insensitivity to eye movements.

We first quantified the neuronal sensitivities to passive vestibular stimulation before and after unilateral labyrinthectomy. Figure 2*Aa* shows the responses of six representative VO neurons to sinusoidal whole body rotations (0.5 Hz, 40 deg s^{-1}). On average, across our population of neurons, sensitivities were comparable for both groups of neurons before labyrinthectomy ~ 0.6 (spk s^{-1})/(deg s^{-1}) [$P = 0.30$; vestibular sensitivities = 0.5 and 0.7 (spk s^{-1})/(deg s^{-1}) for the example type I and II neuron shown in Fig. 2*Aa*, respectively]. Immediately following the lesion (Fig. 2*Aa*, day 1) both groups of neurons showed decreased
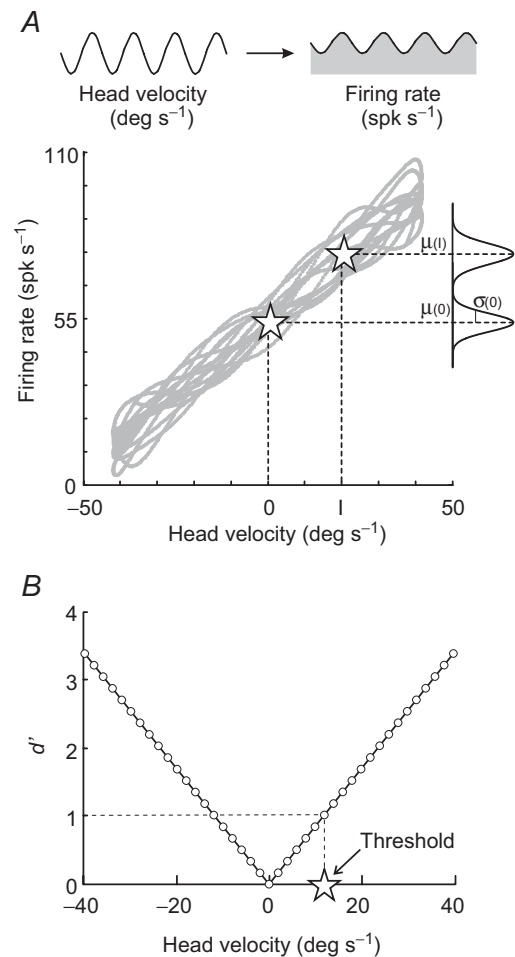

Figure 1. Calculation of neuronal detection thresholds
A, example firing rate *versus* head velocity curve for a vestibular-only neuron. Firing rate distributions with the mean and standard deviation of responses at zero velocity and I = 20 deg s^{-1} are illustrated. *B*, the degree of overlap between two firing rate distributions is measured by *d'*, which varies linearly with head velocity magnitude. Detection thresholds were computed as the velocity at which d' = 1 (star).

sensitivities to vestibular stimulation [0.30 and 0.16 (spk s^{-1})/(deg s^{-1}), for example type I and II neurons, respectively], consistent with the circuitry of the vestibular nuclei as well as our previous findings (Sadeghi *et al.* 2011). This is because both groups of neurons lost the vestibular input that they normally received from the lesioned nerve; for type II neurons, this input is a direct commissural connection, whereas for type I neurons it is mediated mostly via type II neurons (Shimazu & Precht, 1966; Malinvaud *et al.* 2010). Importantly, a few weeks after the lesion the responses of type I neurons showed marked improvement; the example type I neuron (Fig. 2*Aa*, top row, day 28) was typical in that its sensitivity approached normal, pre-lesion values [0.42 (spk s^{-1})/(deg s^{-1})]. In contrast, the response of type II neurons remained reduced even 4 weeks after lesion, as illustrated for the example neuron [Fig. 2*Aa*, bottom row, day 28; 0.23 (spk s^{-1})/(deg s^{-1})].

Figure 2*Ab* summarizes the average neuronal sensitivities before and at different time points after labyrinthectomy for type I and II neurons. Immediately after labyrinthectomy, the response sensitivities were significantly (~70%, $P < 0.001$) reduced from ~0.60 to ~0.20 (spk s^{-1})/(deg s^{-1}) for both groups of neurons. While type I and type II neuronal sensitivities were similar before ($P = 0.30$) and immediately after ($P = 0.31$)

labyrinthectomy, they diverged during the course of compensation ($P = 0.03$, week 1; $P = 0.04$, weeks 2–3; $P < 0.001$, week 3 and after). Notably, the average sensitivity of type I neurons significantly increased over the recovery period (ANOVA; Tukey test; $P < 0.05$) reaching normal values within 4 weeks ($P = 0.81$). In contrast, the average sensitivity of type II neurons did not show significant improvement (ANOVA, $P = 0.40$) over this same period. Note, similar results were obtained for firing rate estimated using either Kaiser (above) or 1/ISI methods.

We next investigated whether and how neuronal thresholds changed over the course of compensation following vestibular lesion. Neuronal detection thresholds are determined by both a neuron's sensitivity and its trial-to-trial variability. If there is no change in neuronal response variability after the lesion, then one would expect that the change in detection thresholds following the lesion would mirror the changes in sensitivity reported above in Fig. 2*Ab*. On the other hand, if neuronal response variability increases after the lesion, then detection thresholds would be adversely affected. To assess these two possibilities, we used signal detection theory to compute the thresholds of single neurons. We first determined the threshold of each individual neuron by plotting its time-dependent firing rate as a function of rotational
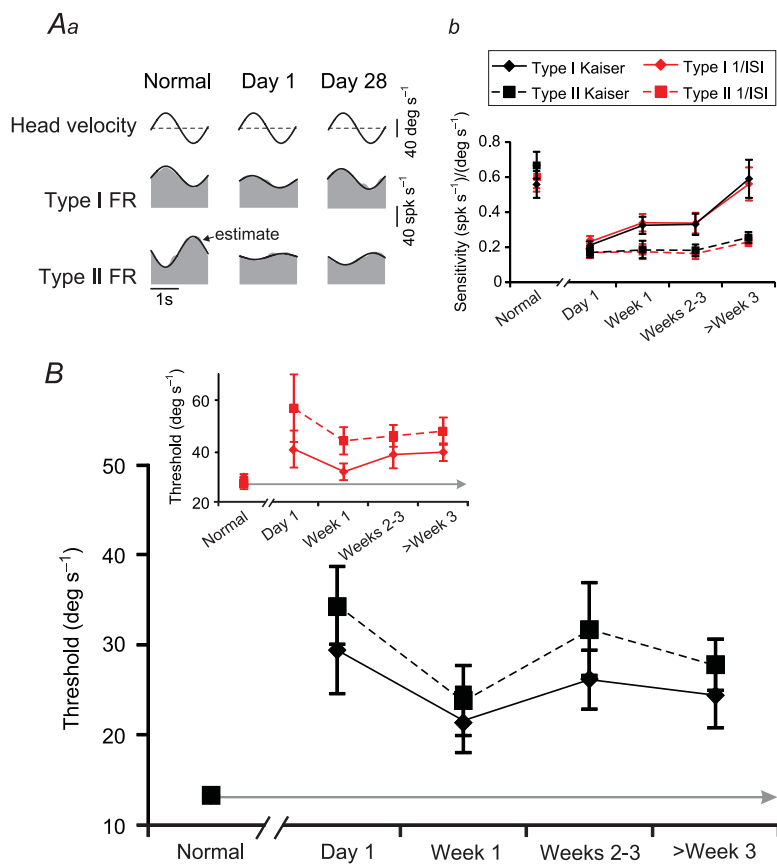

Figure 2. Detection thresholds of vestibular input
A, example of type I and type II VO responses (*Aa*) before, immediately following, and 4 weeks after contralateral labyrinthectomy and population summary (*Ab*) of the changes in vestibular sensitivity of type I (solid) and type II (dashed) VO neurons. Comparable sensitivities were also measured when firing rates were estimated either using the Kaiser filter (black lines) or inverse interspike interval method (red lines). Note that the grey area in (*Aa*) represents the actual firing rate while the overlaying black trace illustrates the 'estimated' firing rate obtained using eqn (1). *B*, summary of the vestibular detection thresholds of type I (solid) and type II (dashed) VO neurons before and throughout the time course of recovery following unilateral labyrinthectomy using either a Kaiser filter (black lines) or the inverse interspike interval (inset: red lines) to estimate firing rate. FR, firing rate; VO, vestibular-only. Error bars indicate S.E.M.

velocity and defining the detection threshold as the lowest absolute velocity value for which $d' = 1$ (see Fig. 1B in Methods). Time-dependent firing rates were estimated using either a Kaiser filter or reciprocal ISI as these two measures could be viewed as representations of firing rate at two opposite ends of the spectrum: (1) extensive filtering using a Kaiser window, and (2) no filtering by using inverse interspike interval (Methods).

Figure 2B summarizes the detection thresholds computed for our population of type I and type II neurons in intact monkeys, and at multiple time points during the first month after unilateral labyrinthectomy. Using the Kaiser filter to estimate firing rate, we found that the average detection thresholds of type I and II neurons before the lesion were both approximately 13 deg s^{-1} (13.9 $\pm$ 1.2 and 13.2 $\pm$ 1.1 deg s^{-1}, respectively) consistent with previous reports (Massot *et al.* 2011). Furthermore, as expected based on neuronal sensitivities, average detection thresholds for both groups of neurons significantly ($P < 0.01$) increased on the first day following unilateral labyrinthectomy (29.4 $\pm$ 4.8 deg s^{-1} and 34.3 $\pm$ 4.3 deg s^{-1} for type I and type II neurons, respectively). Qualitatively similar results were found when we used the inverse interspike interval to compute an estimate of firing rate (inset: detection thresholds of 29.7 $\pm$ 2.8 deg s^{-1} and 27.8 $\pm$ 5.4 deg s^{-1} pre-lesion *versus* 41.3 $\pm$ 7.3 deg s^{-1} and 57.3 $\pm$ 13.3 on day 1 for type I and type II neurons, respectively).

Strikingly, we found that average vestibular detection thresholds for both type I and type II VO neurons did not improve over time but instead remained relatively consistent at these elevated values even more than 3 weeks after unilateral labyrinthectomy (24.4 $\pm$ 3.6 and 27.8 $\pm$ 2.8 deg s^{-1} using the Kaiser filter estimate and 40.4 $\pm$ 3.5 and 48.3 $\pm$ 5.4 deg s^{-1} using the reciprocal ISI estimate for type I and type II VOs, respectively). This trend is similar to that previously reported for self-motion perceptual thresholds in patients (Cousins *et al.* 2013, see Discussion). The lack of improvement in neuronal detection thresholds of type I neurons contrasts strongly, however, with their improved response sensitivity over the same period. Thus, based on this finding we predicted that improvements in response sensitivity after the lesion are accompanied by corresponding increases in neuronal response variability.

Impact of neuronal variability on vestibular detection thresholds during compensation

So far, we have shown that the increase in neuronal detection thresholds observed immediately following labyrinthectomy persisted over the weeks that followed. The fact that type I neurons showed an increase in sensitivity but constant detection threshold suggests

increased trial-to-trial variability is also a feature of the compensation process. In comparison, our results suggest that type II neurons, with persistently lowered sensitivities and correspondingly enhanced thresholds, would not exhibit the same increase in trial-to-trial variability. To test these proposals, we examined the response variability of type I and type II VO neurons to repeated whole body rotations to explore the correlation between neuronal sensitivity and variability after vestibular peripheral loss.

Figure 3A plots the firing rate as a function of head velocity for example type I (left) and type II (right) neurons that showed typical responses for the time frames in which they were recorded: either before (grey curves) or 4 weeks following unilateral labyrinthectomy (blue curves). Interestingly, while the curves for the two examples of type I neurons (Fig. 3A, left) have similar slopes (consistent with the recovery of vestibular sensitivity in type I neurons after unilateral labyrinthectomy), the trial-to-trial variability of the example neuron recorded 4 weeks after vestibular loss was higher; the distribution of firing rates was broader following compensation than before lesion. In contrast, the type II neuron recorded on day 28 (Fig. 3A, right panel, blue curve) was typical in that its sensitivity was lower (compare slopes), and its trial-to-trial variability in the firing rate was similar to that of the example type II neuron recorded pre-lesion (grey curve).

These trends in the trial-to-trial variability of type I *versus* type II neurons were consistent for our population of cells (Fig. 3B). For both groups of neurons, the average firing rate variability before the lesion was ~10 spk s^{-1} during whole body rotations (Fig. 3B, black curves). For type I neurons, increased response variability was observed over the course of compensation, up to ~19 spk s^{-1} (Fig. 3B, solid curves). Type II neurons, in contrast, continued to exhibit equivalent firing rate variability immediately after unilateral labyrinthectomy and throughout the course of vestibular recovery (Fig. 3B, dotted curves), paralleling their consistent sensitivities throughout compensation. Qualitatively similar results were observed using the inverse interspike interval estimation of firing rate (Fig. 3B, inset). Thus, our results show that the improved vestibular sensitivity of type I neurons over the course of vestibular compensation was accompanied by a parallel increase in trial-to-trial variability; and, consequently, neuronal thresholds remained consistently elevated. In contrast, the trial-to-trial response variability of type II neurons remained relatively constant before and after the lesion, and thus consistently elevated neuronal thresholds paralleled the lack of recovery of vestibular sensitivity.

In the analysis above, we determined that the firing rate variability of type I neurons during vestibular stimulation increased and remained elevated after the lesion.

Specifically, we calculated the trial-to-trial variability of responses to sinusoidal stimulation by measuring the standard deviation of the firing rate when stimulation velocity crossed 0 deg s^{-1} [$\sigma(0)$ in Fig. 1A]. We next explored whether trial-to-trial response variability was constant or instead depended on the specific velocity at which this measurement was computed. The variability of the time-dependent firing rate was measured for three velocities (+20 deg s^{-1}, 0 deg s^{-1} and −20 deg s^{-1}) for each type I neuron in the population. Figure 4 illustrates that there was no difference in trial-to-trial firing rate variability as a function of velocity ($P > 0.1$: paired t test with Bonferroni correction). Response variabilities at each velocity similarly increased as a function recovery time. In addition, to rule out the possibility that the changes in variability of type I firing rates might reflect the previously reported results that these neurons tend to have lower baseline firing rates immediately following unilateral labyrinthectomy (Sadeghi *et al.* 2011), we divided each neuron's variability by its mean firing rate at velocity zero. As shown in the inset of Fig. 4, normalized variability measures exhibit the same trend across time as the variability results shown for type I neurons in Fig. 3B. The same was true for type II neurons (data not shown). Thus, response variabilities computed at velocity zero (Fig. 3B and solid black curve in Fig. 4) provided a robust estimate of firing rate variability and are used in all subsequent results.

Detection thresholds of neck proprioceptive inputs

The results shown above demonstrate that while neuronal sensitivities to vestibular stimulation recovered following unilateral peripheral loss, neuronal thresholds remained elevated after the lesion. However, these findings consider the vestibular nuclei as a unimodal structure, as changes in neuronal sensitivities and behavioural performance were only characterized for vestibular stimulation. Indeed, recent studies have demonstrated sensory substitution with extravestibular input (i.e. proprioception) at this first central stage of processing, immediately after vestibular loss (Sadeghi *et al.* 2010, 2011, 2012). Specifically, in natural conditions, the brain has access to proprioceptive as well as vestibular information during self-motion. If neuronal responses to this additional sensory input increase modulation during self-motion, then we might see changes in neuronal thresholds.

To test whether the additional input provided by neck proprioceptors could potentially alter neuronal thresholds for self-motion, we first recorded from single neurons before and after the lesion during a paradigm in which proprioceptive stimulation was delivered in isolation (body-under-head rotation; see Methods). Figure 5Aa illustrates the responses recorded from three example VO neurons while we sinusoidally rotated the monkey's body beneath its earth-stationary head. As previously shown by Roy and Cullen (2001a, 2004), all VO neurons
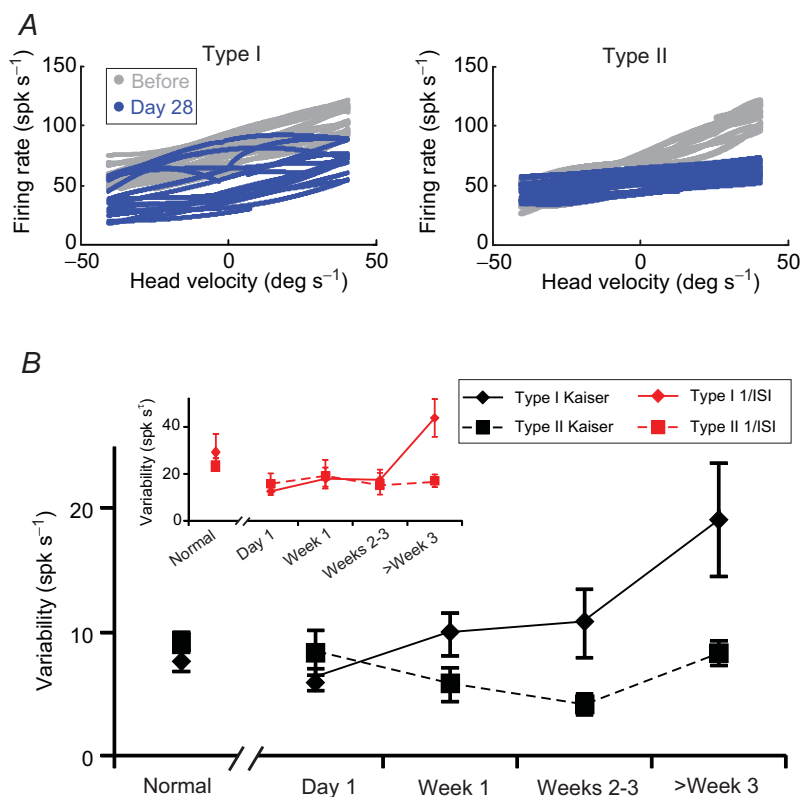

Figure 3. Response variability to vestibular input

A, example of firing rate *versus* head velocity curves for control type I and type II vestibular-only (VO) neurons (grey) and typical type I and type II VO neurons recorded 4 weeks after the lesion (blue). *B*, summary of the changes in neuronal firing rate variabilities of type I (solid) and type II (dashed) VO neurons from normal and several time points after lesion using either a Kaiser filter (black lines) or the inverse interspike interval (inset: red lines) to estimate the firing rate. Type I neurons ($n = 18$, 26, 12, 18, 17 for normal, day 1, week 1, weeks 2–3 and week 3 and after) in diamonds, and type II neurons ($n = 26$, 8, 18, 8, 28 for normal, day 1, week 1, weeks 2–3 and week 3 and after) in squares. Error bars indicate s.e.m.

were unresponsive to passive stimulation of neck proprioceptors before labyrinthectomy. In contrast, immediately following labyrinthectomy, ~40% of type I and II neurons (13 of 34) showed robust modulation [i.e. sensitivity greater than 0.1 (spk s^{-1})/(deg s^{-1})]. Moreover, by day 28, >70% of neurons (23 of 30) were sensitive to neck proprioceptive stimulation.

Figure 5*Ab* shows the average neck proprioceptive sensitivities as a function of time for our samples of type I and type II neurons. Notably, neck sensitivities peaked just after labyrinthectomy and remained elevated. We next estimated the detection thresholds of the neck responsive neurons during proprioceptive stimuli delivered in isolation. We found that neuronal thresholds for proprioceptive stimulation remained constant at ~30 deg s^{-1} for both type I and II neurons (Fig. 5*B*). Interestingly, this value is comparable to neuronal motion detection thresholds for vestibular stimulation after unilateral vestibular loss (i.e. Fig. 2*B*). Because both neuronal sensitivities and thresholds measured during proprioceptive stimulation remained constant during compensation, we predicted that neuronal trial-to-trial variability should likewise remain constant over the same period. Indeed, our results show that the neuronal firing rate variability during neck proprioceptive stimulation remained constant at ~8 spk s^{-1} across time for both type I and type II neurons (Fig. 5*C*). Finally, comparison of results using the inverse interspike interval to estimate firing rate revealed comparable trends for neuronal sensitivities, detection thresholds and response variability to those obtained here using the Kaiser filter based estimate (Fig. 5*Ab* and insets in Fig. 5*B* and *C* respectively).

Sensory integration in the recovery of neural detection thresholds

As described above, we observed sensory substitution with proprioceptive input after the strength of the vestibular sensory input was reduced by unilateral labyrinthectomy. As such, we hypothesized that neck proprioception may play a role in self-motion perception when vestibular input is reduced because of unilateral vestibular lesion. Accordingly, we next measured neuronal responses during passive head-on-body rotations in which movement of the head relative to space stimulated the vestibular sensors while rotation of the head relative to the body activated proprioceptors in the neck musculature (Fig. 6*A*, right column). For the purpose of this analysis, type I and II neurons were considered collectively because they encoded similar neck signals over the course of compensation (Fig. 5).

Two example neurons are shown in Fig. 6*A*. To quantify neuronal detection thresholds when both vestibular and proprioception cues were available, we first considered neurons with complementary responses to these stimuli when each was applied in isolation (i.e. agonistic neurons, Fig. 6*A*). If integration of a given neuron's responses for the two modalities (e.g. Fig. 6*A*, left and centre columns) is performed by a simple linear summation of unisensory activity, then matching multimodal stimuli should elicit greater modulation. Consistent with the previous report of Sadeghi *et al.* (2011), linear summation provided an excellent prediction (Fig. 6*A*, right column, top grey row; red dashed line, VAF = 0.73) of response sensitivity during combined stimulation, which was comparable to the actual best fit (thick black line, VAF = 0.76). We further tested whether the increase in modulation was associated with an improvement in neuronal detection thresholds in the combined condition. Indeed, threshold values were significantly improved for synchronous stimulation with vestibular and proprioception cues as compared to the application of vestibular stimulation alone for both Kaiser ($P = 0.048$) and reciprocal ISI ($P = 0.01$) firing rate estimation methods (Fig. 6*B*, compare grey bars with dashed lines).

We next considered neurons with opposing responses to the two stimuli (i.e. antagonistic neurons: Fig. 6*A*,

Figure 4. Variability is consistent across rotational velocities and changes are not explained by changes in mean firing rate
Comparison of firing rate variability measurements taken from the distributions of firing rates of type I vestibular-only neurons at +20 deg s^{-1}, 0 deg s^{-1} and −20 deg s^{-1} whole body rotation. Throughout the course of recovery following unilateral labyrinthectomy, there is no difference between the three measurements. Inset: trend in firing rate variability over time following lesion, after measurements were normalized by the mean firing rate of each neuron at 0 deg s^{-1}. Error bars indicate S.E.M.
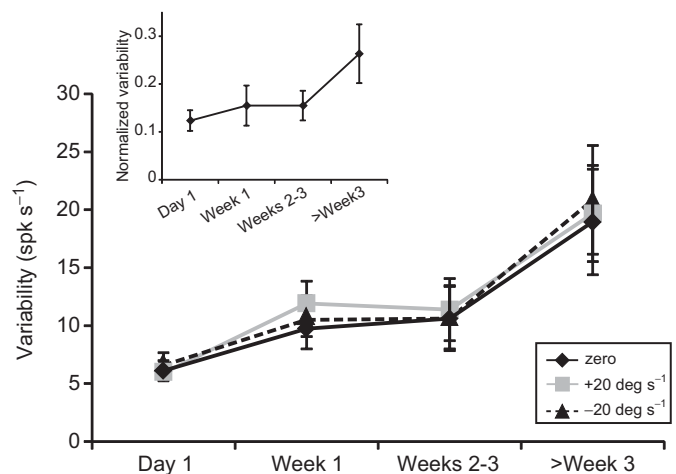
bottom grey row; compare left and centre columns). In this case, simple linear summation of unisensory activity predicted reduced modulation for matching multimodal stimulation – a prediction again confirmed by the similarity of the predicted response and actual best fit (Fig. 6*A*, right column, bottom grey row; compare red dashed and thick black lines, VAF = 0.84 *versus* 0.85, respectively). This led us to hypothesize that antagonistic neurons might have correspondingly worse (i.e. elevated) detection thresholds in the combined condition, as compared to the condition in which vestibular input was applied alone. Indeed, we found that neuronal detection thresholds were higher during combined than vestibular stimulation alone (Fig. 6*B*, compare white bars with dashed lines). This difference was significant when the firing rate was estimated with the Kaiser method ($P = 0.01$), but not when the more noisy reciprocal

ISI method was used ($P = 0.12$). Taken together, our results show that a distinct subclass of neurons, which have complementary neck proprioceptive and vestibular responses, show improvements in detection thresholds during combined as compared to VO stimulation. The implications of these results for the functional recovery of patients are discussed below.

Discussion

In the present study, we investigated the changes in neural thresholds that occur following unilateral vestibular loss. The ability to distinguish between leftward/rightward motion (as quantified by direction–discrimination thresholds) is significantly compromised in patients immediately after vestibular loss (Cutfield *et al.* 2011), and remains substandard even following compensation
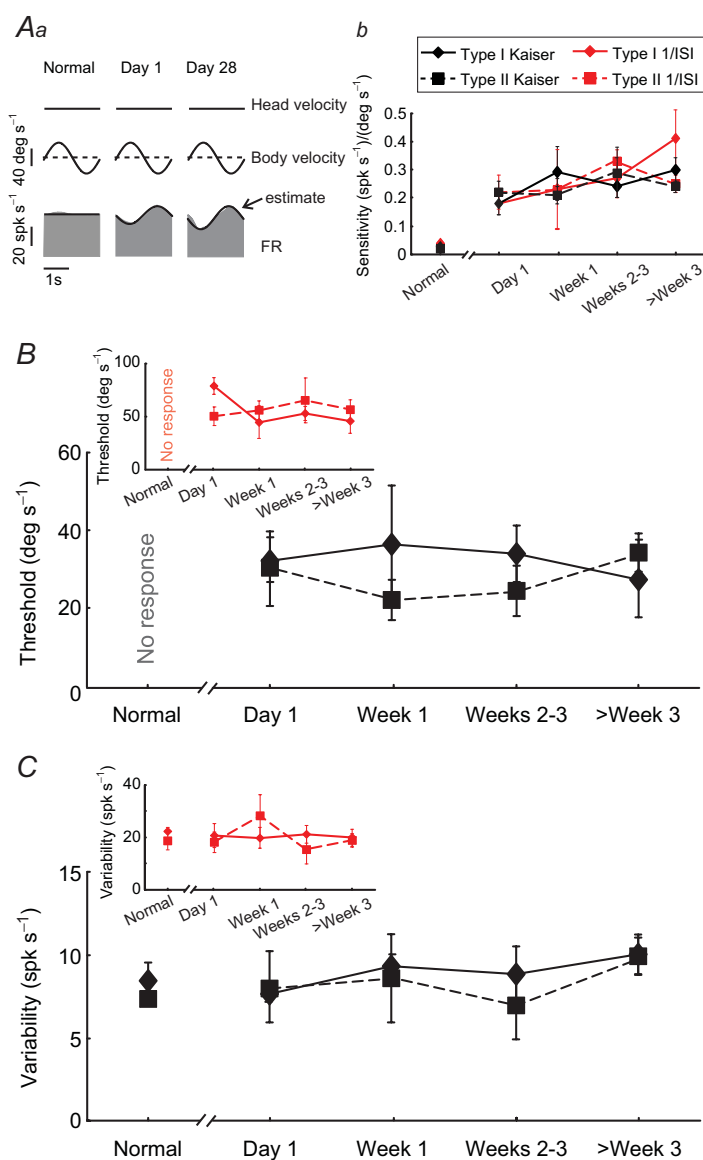

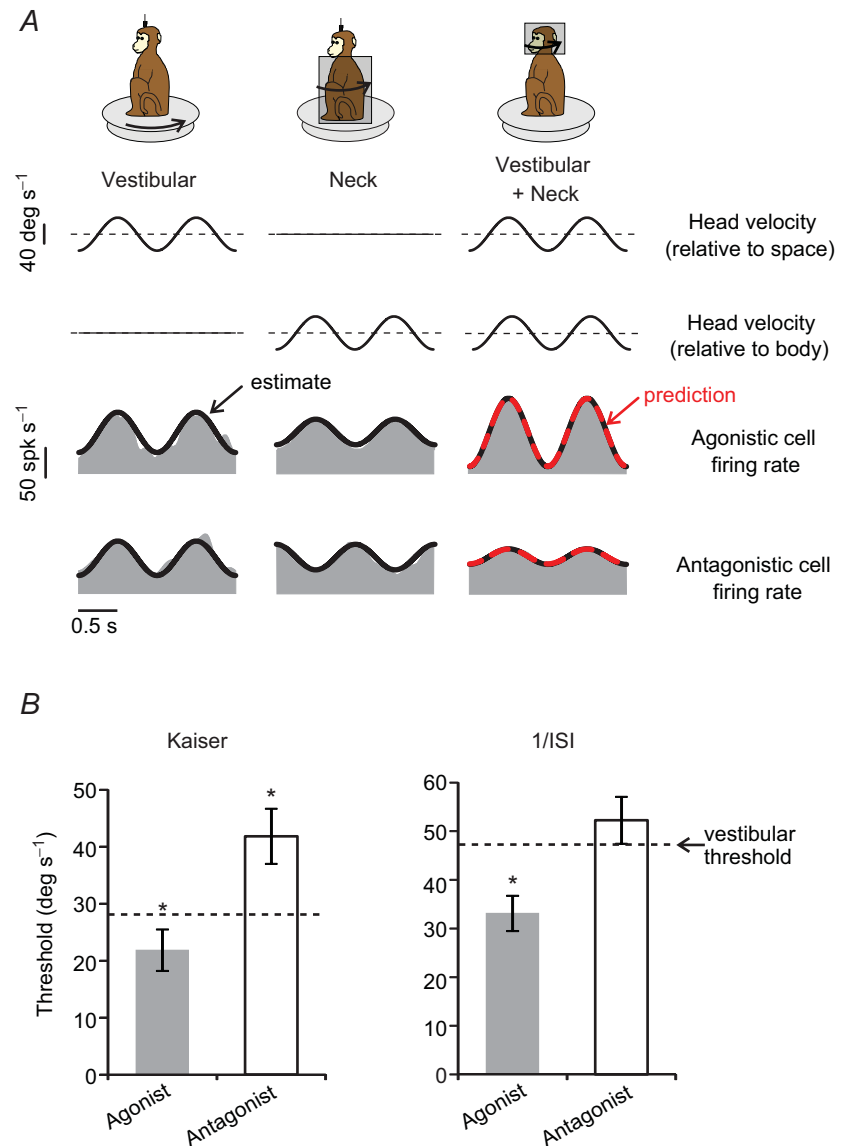**Figure 5. Detection thresholds of neck proprioceptive input**

A, example neural responses (*Aa*) and population response summary (*Ab*) during neck proprioceptive stimulation. While vestibular-only neurons recorded from intact animals were not responsive, ~40% and >70% of neurons recorded immediately and 4 weeks following lesion showed clear modulation, respectively. *B* and *C*, average detection thresholds (*B*), and response variability (*C*) during neck proprioceptive stimulation of neck sensitive type I (solid) and type II (dashed) neurons using a Kaiser filter (black lines) or the inverse interspike interval (insets: red lines) to estimate firing rate. Note that the variability of the response during the normal condition (where there is no modulation) was comparable to that observed in the driven state following vestibular lesion. FR, firing rate.

(Cousins *et al.* 2013). Here, we quantified the neural basis of the elevation of detection thresholds after unilateral vestibular loss by recording from individual neurons in rhesus monkeys. We focused on neurons at the first central stage of vestibular processing, which receive input from vestibular afferents and in turn contribute to the computation of spatial orientation as well as self-motion perception through their interconnections with the vestibular thalamus and cerebellum. We first found that both type I and type II neuronal detection thresholds for vestibular stimulation show a marked (~120%) increase immediately following vestibular loss. Furthermore, neuronal thresholds showed no significant improvement (84% elevated relative to control values >1 month). We then found that for type I neurons, the lack of improvement in neuronal detection thresholds, despite recovery of neuronal sensitivity, could be explained

by the strong correlation between increases in response sensitivity and response variability during compensation. For type II neurons, however, thresholds, which increase with the drop in sensitivity immediately following labyrinthectomy, remain elevated due to no further significant change in sensitivity or variability during the time course of compensation. Overall, the observed trend for neuronal thresholds mirrors the time course of perceptual thresholds in patients (Cousins *et al.* 2013), and thus provides a neural correlate for the sustained impaired behavioural performance following vestibular lesion.

In addition, we found that extravestibular proprioceptive signals that are unmasked during compensation (i.e. the synapses of proprioceptive inputs onto vestibular nuclei neurons were silent before the lesion but became responsive to neck stimulation after the lesion; see

Figure 6. Detection thresholds during passive stimulation of vestibular and neck proprioceptive sensors
A, activity of two example vestibular-only neurons (two bottom rows: agonistic and antagonistic neurons, respectively) during 1 Hz sinusoidal passive head-on-body rotations. The two example neurons showed similar sensitivities to vestibular stimulation (left column: whole-body rotation) as well as comparable but opposite sign sensitivities to neck stimulation (middle column: body-under-head rotation). Accordingly, linear summation of these two sensitivity components resulted in a greater overall sensitivity for the agonistic neuron compared to the antagonistic neuron during 'vestibular + neck' stimulation (right column: head-on-body rotation). Linear summation of response sensitivities during individual stimulation of vestibular and neck sensors provided a prediction (red dashed line) comparable to the best fit estimation during the head-on-body rotations (thick black line). *B*, population-averaged neuronal thresholds for agonistic and antagonistic neurons following labyrinthectomy. Agonist neurons display a lower threshold for head-on-body motion (grey bar) as compared to whole body rotation (vestibular stimulation: dashed line), the converse is true for antagonist neurons (compare white bar with dashed line). Similar results were obtained when either Kaiser filter (left) or inverse interspike interval (right) methods were used to estimate firing rate. Error bars indicate s.e.m. *P < 0.05.

Sadeghi *et al.* 2010, 2011, 2012) can improve thresholds for self-motion detection at the level of individual neurons. Notably, the unmasking of neck proprioceptive inputs produced a relative improvement in threshold for neurons with complementary sensitivities to vestibular and neck proprioceptive stimulation for motion that was generated by rotations of the head on body (rather than head and body together in space). These results provide a neural correlate for the patient benefits provided by rehabilitative strategies incorporating movements that produce multimodal (i.e. combined vestibular and proprioceptive) stimulation. Taken together, our data show that improvements in self-motion detection following vestibular loss can be enhanced by the reweighting of extravestibular inputs, but are ultimately constrained by increases in response variability to vestibular inputs at the level of the first central stage of vestibular processing.

Neuronal thresholds show less recovery than response sensitivities after vestibular loss

The neurons recorded in the present study are known to respond robustly to head motion in normal conditions (Fuchs & Kimm, 1975; Chubb *et al.* 1984; Scudder & Fuchs, 1992; Cullen & McCrea, 1993; Boyle *et al.* 1996; McCrea *et al.* 1999; Cullen *et al.* 2001; Zhou *et al.* 2006). Previous reports have further shown that neuronal sensitivities to vestibular inputs in monkeys decrease immediately following unilateral vestibular loss (Sadeghi *et al.* 2011). Furthermore, as confirmed in the present report, the sensitivities of type I neurons recover within a few weeks, reaching values that are close to those measured before the lesion (Sadeghi *et al.* 2011; Newlands & Wei, 2013).

In conditions where vestibular function is intact, these same neurons have rotational detection thresholds on the order of ~15 deg s^{-1} when computed with an optimal Kaiser filter (Massot *et al.* 2011). In the present study we found that the rotational detection thresholds increased by approximately two-fold to ~30 deg s^{-1} following unilateral labyrinthectomy, but (unlike neuronal sensitivities) did not significantly improve over time. We used a Kaiser filter to obtain a lower bound estimate of neuronal thresholds (see also Yu *et al.* 2012; Jamali *et al.* 2013), but emphasize that a comparable percentage increase in rotational detection threshold was also computed using the 1/ISI representation of neuronal firing rate (84% *vs.* 66% following compensation for Kaiser and 1/ISI, respectively).

Time course of neuronal detection thresholds *versus* functional recovery

The vestibular nuclei neurons that were the focus of the present study receive inputs from the vestibular nerve and, in turn, mediate vestibulospinal reflexes via their projections to the spinal cord (Wilson *et al.* 1990; Boyle, 1993; Boyle *et al.* 1996; Gdowski & McCrea, 1999). These neurons also project to higher-order centres such as the thalamus and cortex (Meng *et al.* 2007; Marlinski & McCrea, 2008*a,b*), and are thought to carry information relevant for perception of self-motion and spatial orientation. Changes in the vestibular sensitivities of these neurons parallel the functional recovery of the efficacy of vestibulospinal reflexes following unilateral vestibular loss (reviewed in Smith & Curthoys, 1989). In contrast, the results of the present study reveal a markedly different trend in neuronal detection thresholds. We found that while neuronal detection thresholds also worsen immediately following the lesion, they show little improvement during compensation (i.e. 1–2 months after lesion). A question then naturally arises: Why should reflexes correlate better with sensitivity rather than neuronal thresholds? We note that the efficacy of reflexes is typically characterized using suprathreshold stimuli and thus is probably less affected by the variability in the sensory neurons' responses. Importantly, however, we would expect that the threshold of vestibular reflexes (e.g. as measured in Seemungal *et al.* 2004; Haburcakova *et al.* 2012) would be affected by neuronal variability and thus remain worse than normal after a vestibular lesion. Interestingly, in a recent report, Cousins *et al.* (2013) showed that both VOR thresholds and perceptual thresholds increase after a unilateral vestibular lesion, and despite some slight recovery remain elevated even after ~10 weeks. Further work is needed to understand the effect of the increased variability observed in the present study on perceptual *versus* reflex thresholds.

The time course of neuronal thresholds is analogous to the trend reported for patients' perception (Cousins *et al.* 2013). Specifically, patients' perceptual thresholds for rotation increase from ~8 deg s^{-1} to ~20 deg s^{-1} immediately (i.e. within 1–2 days) following loss of vestibular function (Cutfield *et al.* 2011) and do not recover to near-normal values even after 10 weeks (Cousins *et al.* 2013). We note that Cousins *et al.* (2013) reported significant improvements (i.e. lower thresholds) over the course of recovery for a subset of patients, but that these individuals had minimal canal paresis, indicating that their peripheral vestibular input was still largely intact. Moreover, patients with severe unilateral vestibular loss can show limitations in other aspects of their functional recovery (e.g. impaired VOR and subjective visual vertical perception; reviewed in Dutia, 2010). Further experiments will be required to investigate fully the relationship between the level of injury and the extent of compensation. We speculate that the increase in neuronal firing rate variability, which occurs during compensation and in turn accounts for the lack of improvement of detection thresholds, may ultimately also

have effects on the accuracy of other vestibular-dependent behaviours.

Functional implications of neuronal response variability

Variability of neuronal spiking activity is an important factor in neural coding (Stein *et al.* 2005; McDonnell & Ward, 2011). There is accumulating evidence that neural variability should be taken into account to fully understand neural coding strategies in early sensory processing (e.g. Chacron *et al.* 2005; Sadeghi *et al.* 2007*a*). We have recently shown a strong positive correlation between vestibular afferent sensitivity and variability in the otolith system (Jamali *et al.* 2013). Specifically, in the stimulated condition the ratio of these two quantities (i.e. response variability/sensitivity, which corresponds to the neuronal threshold), remains approximately constant. It is noteworthy that correlations between response variability and sensitivity are not unique to the otolith system. For instance they have been reported in other systems (e.g. auditory, Kiang *et al.* 1965; Tollin *et al.* 2008) and thus are probably a general feature of sensory processing.

Our present results indicate that following unilateral lesion of the labyrinth, both sensitivity and variability of responses to vestibular input increase. As we recently proposed for otolith afferents (Jamali *et al.* 2013), a source of noise corresponding to the 'sensory noise' and 'cellular noise' categories as described by Faisal *et al.* (2008) could contribute to the increases in neuronal variability of vestibular nuclei neurons observed following labyrinthectomy. This noise can originate from sensory transduction as well as from intrinsic properties (Smith & Goldberg, 1986; Kalluri *et al.* 2010), and thus will become greater at the level of the vestibular nuclei after unilateral lesion because of the overall increased system gain. In addition, the unmasking of neck proprioceptive inputs may also serve as a source of noise. In particular, this newly substituted sensory input could potentially cause extra fluctuations in the cell membrane thereby contributing to larger firing rate variability. Additional studies will be needed to assess the extent to which each of these two potential noise sources contributes to increases in neuronal variability of vestibular nuclei neurons following labyrinthectomy.

Role of extravestibular inputs in vestibular-only rotational detection thresholds

It is generally accepted that sensory systems have evolved to accommodate the uncertainty of their inputs. This uncertainty is the result of the intrinsic physical properties of sensory stimuli (for example, statistical variations in photon arrival at the retina) as well as the noise inherent to the transformation of physical stimuli into neuro-

nal activity (reviewed in Fetsch *et al.* 2013). In everyday life, however, sensory stimuli are most commonly sensed with more than a single modality. Thus, to overcome the constraints of sensory uncertainty on behavioural performance, the brain can combine sensory information across modalities. For example, vestibulospinal reflexes are dependent on whether sensory feedback is congruent with the motor-generated expectation to balance the body (Luu *et al.* 2012). Such multisensory cue integration is particularly vital when the fidelity of one sensory input has been compromised.

For instance, in the present study, neurons in the vestibular nuclei lost the afferent input that they normally receive from the lesioned nerve (i.e. via direct connections or indirect commissural connections between the two vestibular nuclei). The resulting loss of information triggers neuronal plasticity (e.g. homeostatic changes), which is, in part, reflected as an increase in the sensitivity to neck proprioceptive inputs (Sadeghi *et al.* 2010, 2011, 2012). While the mechanism underlying the sensory substitution with proprioceptive input is not known, previous studies have shown that vestibular and proprioceptive inputs to vestibular nuclei neurons are mediated by AMPA and NMDA receptors, respectively (Smith *et al.* 1991; Straka & Dieringer, 2004). We speculate that after the lesion, an increase in the number of AMPA but not NMDA receptors (King *et al.* 2002) enhances the co-localization of NMDA and AMPA receptors (Chen *et al.* 2000), thereby resulting in activation of 'silent' NMDA synapses (Kerchner & Nicoll, 2008).

Importantly, because of this sensory substitution, the brain has access to a pool of neurons (i.e. agonistic neurons, Fig. 7*A*) for which multisensory integration leads to better detection of self-motion (Fig. 7*B*). Thus, sensory substitution at the earliest stages of vestibular processing and resultant multisensory interactions may be fundamental to augment our sense of self-motion after vestibular loss. Indeed, it has been shown that vestibular patients rely more strongly on proprioception to compensate for their injury (Betts *et al.* 2000; Peterka *et al.* 2011). In addition, while neck proprioceptive inputs play a negligible role in gaze stabilization in normal animals, their influence becomes significant following vestibular loss (Dichgans *et al.* 1973; Newlands *et al.* 1999). Interestingly, Sadeghi *et al.* (2010, 2011) showed that unmasking of neck proprioceptive inputs at the level of individual neurons played a critical role in the early stages of vestibular compensation, demonstrated by the earlier and more significant recovery of vestibular responses for neurons sensitive to neck proprioception.

We further emphasize that while there is impressive compensation in the first month after unilateral vestibular loss, full compensation can require months or even years. The mechanisms underlying compensation are multifaceted; while activation of silent synapses (i.e. neck

proprioceptive) provides a substrate for multisensory integration, it is only one aspect of functional recovery after vestibular lesion. Other documented mechanisms include changes in the synaptic efficacy or intrinsic excitability of vestibular neurons (Him and Dutia, 2001) as well as a shift in the proportion of phasic/tonic neuronal population (Beraneck & Idoux, 2012). Finally, more global changes in oculomotor and postural strategies can facilitate recovery from vestibular loss (e.g. Peng *et al.* 2005; Horak, 2010).

Our results provide a neural correlate for the observation that improvements in balance and self-motion perception can be achieved by strategies that effectively incorporate multimodal (i.e. combined vestibular and proprioceptive) stimulation into rehabilitative training. For example, common rehabilitation procedures such as Cawthorne–Cooksey exercises involve head and body movements, as well as well as eye–head co-ordination and balance tasks to promote compensation (reviewed in Ricci *et al.* 2010). Future experiments will be needed to further our understanding of the mechanisms that underlie the observed sensory substitution with extravestibular (i.e. proprioceptive) inputs in vestibular pathways following vestibular sensory loss.

Figure 7. Contribution of vestibular and neck inputs to agonistic VO detection thresholds
A, schematic outlining the proposed role of neck proprioceptive inputs in contributing to VO neuronal detection thresholds following unilateral labyrinthectomy. *B*, comparison of population-averaged neuronal thresholds of agonistic VO neurons during whole body rotations (vestibular; blue), body-under-head rotations (neck proprioception; red) and head-on-body rotations (sum; purple) in the normal condition, and within 1 week and >1 week following unilateral labyrinthectomy. Shading indicates s.e.m. VO, vestibular-only.

References

Beraneck M & Idoux E (2012). Reconsidering the role of neuronal intrinsic properties and neuromodulation in vestibular homeostasis. *Front Neurol* **3**, 25.

Betts GA, Barone M, Karlberg M, MacDougall H & Curthoys IS (2000). Neck muscle vibration alters visually-perceived roll after unilateral vestibular loss. *NeuroReport* **11**, 2659–2662.

Boyle R (1993). Activity of medial vestibulospinal tract cells during rotation and ocular movement in the alert squirrel monkey. *J Neurophysiol* **70**, 2176–2180.

Boyle R, Belton T & McCrea RA (1996). Responses of identified vestibulospinal neurons to voluntary eye and head movements in the squirrel monkey. *Ann N Y Acad Sci* **781**, 244–263.

Chacron MJ, Maler L & Bastian J (2005). Electroreceptor neuron dynamics shape information transmission. *Nat Neurosci* **8**, 673–678.

Chaudhuri SE, Karmali F & Merfeld DM (2013). Whole-body motion-detection tasks can yield much lower thresholds than direction-recognition tasks: implications for the role of vibration. *J Neurophysiol* **110**, 2764–2772.

Chen LW, Yung KK & Chan YS (2000). Co-localization of NMDA receptors and AMPA receptors in neurons of the vestibular nuclei of rats. *Brain Res* **884**, 87–97.

Cherif S, Cullen KE & Galiana HL (2008). An improved method for the estimation of firing rate dynamics using an optimal digital filter. *J Neurosci Methods* **173**, 165–181.

Chubb MC, Fuchs AF & Scudder CA (1984). Neuron activity in monkey vestibular nuclei during vertical vestibular stimulation and eye movements. *J Neurophysiol* **52**, 724–742.

Cousins S, Kaski D, Cutfield N, Seemungal B, Golding JF, Gresty M, Glasauer S & Bronstein AM (2013). Vestibular perception following acute unilateral vestibular lesions. *PLoS One* **8**, e61862.

Cullen KE (2012). The vestibular system: multimodal integration and encoding of self-motion for motor control. *Trends Neurosci* **35**, 185–196.

Cullen KE & McCrea RA (1993). Firing behavior of brain stem neurons during voluntary cancellation of the horizontal vestibuloocular reflex. I. Secondary vestibular neurons. *J Neurophysiol* **70**, 828–843.

Cullen KE, Chen-Huang C & McCrea RA (1993). Firing behavior of brain stem neurons during voluntary cancellation of the horizontal vestibuloocular reflex. II. Eye movement related neurons. *J Neurophysiol* **70**, 844–856.

Cullen KE, Rey CG, Guitton D & Galiana HL (1996). The use of system identification techniques in the analysis of oculomotor burst neuron spike train dynamics. *J Comput Neurosci* **3**, 347–368.

Cullen KE, Roy JE & Sylvestre PA (2001). Signal processing by vestibular nuclei neurons is dependent on the current behavioral goal. *Ann N Y Acad Sci* **942**, 345–363.

Cutfield NJ, Cousins S, Seemungal BM, Gresty MA & Bronstein AM (2011). Vestibular perceptual thresholds to angular rotation in acute unilateral vestibular paresis and with galvanic stimulation. *Ann N Y Acad Sci* **1233**, 256–262.
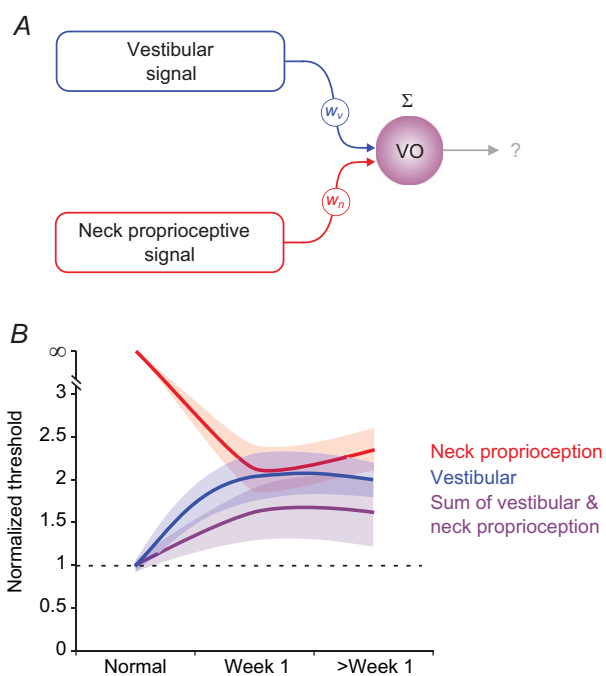
Dichgans J, Bizzi E, Morasso P & Tagliasco V (1973). Mechanisms underlying recovery of eye–head coordination following bilateral labyrinthectomy in monkeys. *Exp Brain Res* **18**, 548–562.

Dutia MB (2010). Mechanisms of vestibular compensation: recent advances. *Curr Opin Otolaryngol Head Neck Surg* **18**, 420–424.

Faisal AA, Selen LP & Wolpert DM (2008). Noise in the nervous system. *Nat Rev Neurosci* **9**, 292–303.

Fetsch CR, DeAngelis GC & Angelaki DE (2013). Bridging the gap between theories of sensory cue integration and the physiology of multisensory neurons. *Nat Rev Neurosci* **14**, 429–442.

Fuchs AF & Kimm J (1975). Unit activity in vestibular nucleus of the alert monkey during horizontal angular acceleration and eye movement. *J Neurophysiol* **38**, 1140–1161.

Fuchs AF & Robinson DA (1966). A method for measuring horizontal and vertical eye movement chronically in the monkey. *J Appl Physiol* **21**, 1068–1070.

Gdowski GT & McCrea RA (1999). Integration of vestibular and head movement signals in the vestibular nuclei during whole-body rotation. *J Neurophysiol* **82**, 436–449.

Grabherr L, Nicoucar K, Mast FW & Merfeld DM (2008). Vestibular thresholds for yaw rotation about an earth-vertical axis as a function of frequency. *Exp Brain Res* **186**, 677–681.

Green DM & Swets JA. *Signal Detection Theory and Psychophysics*. New York: Wiley, 1966, pp. xi, 455.

Haburcakova C, Lewis RF & Merfeld DM (2012). Frequency dependence of vestibuloocular reflex thresholds. *J Neurophysiol* **107**, 973–983.

Hayes AV, Richmond BJ & Optican LM (1982). A UNIX-based multiple process system for real-time data acquisition and control. *WESCON Conf Proc* **2**, 1–10.

Him A & Dutia MB (2001). Intrinsic excitability changes in vestibular nucleus neurons after unilateral deafferentation. *Brain Res* **908**, 58–66.

Horak FB (2010). Postural compensation for vestibular loss and implications for rehabilitation. *Restor Neurol Neurosci* **28**, 57–68.

Huterer M & Cullen KE (2002). Vestibuloocular reflex dynamics during high-frequency and high-acceleration rotations of the head on body in rhesus monkey. *J Neurophysiol* **88**, 13–28.

Jamali M, Sadeghi SG & Cullen KE (2009). Response of vestibular nerve afferents innervating utricle and saccule during passive and active translations. *J Neurophysiol* **101**, 141–149.

Jamali M, Carriot J, Chacron MJ & Cullen KE (2013). Strong correlations between sensitivity and variability give rise to constant discrimination thresholds across the otolith afferent population. *J Neurosci* **33**, 11302–11313.

Judge SJ, Richmond BJ & Chu FC (1980). Implantation of magnetic search coils for measurement of eye position: an improved method. *Vision Res* **20**, 535–538.

Kalluri R, Xue J & Eatock RA (2010). Ion channels set spike timing regularity of mammalian vestibular afferent neurons. *J Neurophysiol* **104**, 2034–2051.

Kerchner GA & Nicoll RA (2008). Silent synapses and the emergence of a postsynaptic mechanism for LTP. *Nat Rev Neurosci* **9**, 813–825.

Kiang NY, Pfeiffer RR, Warr WB & Backus AS (1965). Stimulus coding in the cochlear nucleus. *Trans Am Otol Soc* **53**, 35–58.

King J, Zheng Y, Liu P, Darlington CL & Smith PF (2002). NMDA and AMPA receptor subunit protein expression in the rat vestibular nucleus following unilateral labyrinthectomy. *NeuroReport* **13**, 1541–1545.

Luu BL, Inglis JT, Huryn TP, Van der Loos HF, Croft EA & Blouin JS (2012). Human standing is modified by an unconscious integration of congruent sensory and motor signals. *J Physiol* **590**, 5783–5794.

Malinvaud D, Vassias I, Reichenberger I, Rossert C & Straka H (2010). Functional organization of vestibular commissural connections in frog. *J Neurosci* **30**, 3310–3325.

Mallery RM, Olomu OU, Uchanski RM, Militchin VA & Hullar TE (2010). Human discrimination of rotational velocities. *Exp Brain Res* **204**, 11–20.

Marlinski V & McCrea RA (2008*a*). Activity of ventroposterior thalamus neurons during rotation and translation in the horizontal plane in the alert squirrel monkey. *J Neurophysiol* **99**, 2533–2545.

Marlinski V & McCrea RA (2008*b*). Coding of self-motion signals in ventro-posterior thalamus neurons in the alert squirrel monkey. *Exp Brain Res* **189**, 463–472.

Massot C, Chacron MJ & Cullen KE (2011). Information transmission and detection thresholds in the vestibular nuclei: single neurons vs. population encoding. *J Neurophysiol* **105**, 1798–1814.

McCrea RA, Gdowski GT, Boyle R & Belton T (1999). Firing behavior of vestibular neurons during active and passive head movements: vestibulo-spinal and other non-eye-movement related neurons. *J Neurophysiol* **82**, 416–428.

McDonnell MD & Ward LM (2011). The benefits of noise in neural systems: bridging theory and experiment. *Nat Rev Neurosci* **12**, 415–426.

Meng H, May PJ, Dickman JD & Angelaki DE (2007). Vestibular signals in primate thalamus: properties and origins. *J Neurosci* **27**, 13590–13602.

Newlands SD & Wei M (2013). Responses of central vestibular neurons to sinusoidal yaw rotation in compensated macaques after unilateral labyrinthectomy. *J Neurophysiol* **110**, 1822–1836.

Newlands SD, Ling L, Phillips JO, Siebold C, Duckert L & Fuchs AF (1999). Short- and long-term consequences of canal plugging on gaze shifts in the rhesus monkey. I. Effects on gaze stabilization. *J Neurophysiol* **81**, 2119–2130.

Peng GC, Minor LB & Zee DS (2005). Gaze position corrective eye movements in normal subjects and in patients with vestibular deficits. *Ann N Y Acad Sci* **1039**, 337–348.

Peterka RJ, Statler KD, Wrisley DM & Horak FB (2011). Postural compensation for unilateral vestibular loss. *Front Neurol* **2**, 57.

Ricci NA, Aratani MC, Dona F, Macedo C, Caovilla HH & Gananca FF (2010). A systematic review about the effects of the vestibular rehabilitation in middle-age and older adults. *Rev Bras Fisioter* **14**, 361–371.

Robinson DA (1970). Oculomotor unit behavior in the monkey. *J Neurophysiol* **33**, 393–403.

Roy JE & Cullen KE (2001*a*). Passive activation of neck proprioceptive inputs does not influence the discharge patterns of vestibular nuclei neurons. *Ann N Y Acad Sci* **942**, 486–489.

Roy JE & Cullen KE (2001*b*). Selective processing of vestibular reafference during self-generated head motion. *J Neurosci* **21**, 2131–2142.

Roy JE & Cullen KE (2004). Dissociating self-generated from passively applied head motion: neural mechanisms in the vestibular nuclei. *J Neurosci* **24**, 2102–2111.

Sadeghi SG, Minor LB & Cullen KE (2006). Dynamics of the horizontal vestibuloocular reflex after unilateral labyrinthectomy: response to high frequency, high acceleration, and high velocity rotations. *Exp Brain Res* **175**, 471–484.

Sadeghi SG, Chacron MJ, Taylor MC & Cullen KE (2007*a*). Neural variability, detection thresholds, and information transmission in the vestibular system. *J Neurosci* **27**, 771–781.

Sadeghi SG, Minor LB & Cullen KE (2007*b*). Response of vestibular-nerve afferents to active and passive rotations under normal conditions and after unilateral labyrinthectomy. *J Neurophysiol* **97**, 1503–1514.

Sadeghi SG, Mitchell DE & Cullen KE (2009). Different neural strategies for multimodal integration: comparison of two macaque monkey species. *Exp Brain Res* **195**, 45–57.

Sadeghi SG, Minor LB & Cullen KE (2010). Neural correlates of motor learning in the vestibulo-ocular reflex: dynamic regulation of multimodal integration in the macaque vestibular system. *J Neurosci* **30**, 10158–10168.

Sadeghi SG, Minor LB & Cullen KE (2011). Multimodal integration after unilateral labyrinthine lesion: single vestibular nuclei neuron responses and implications for postural compensation. *J Neurophysiol* **105**, 661–673.

Sadeghi SG, Minor LB & Cullen KE (2012). Neural correlates of sensory substitution in vestibular pathways following complete vestibular loss. *J Neurosci* **32**, 14685–14695.

Scudder CA & Fuchs AF (1992). Physiological and behavioral identification of vestibular nucleus neurons mediating the horizontal vestibuloocular reflex in trained rhesus monkeys. *J Neurophysiol* **68**, 244–264.

Seemungal BM, Gunaratne IA, Fleming IO, Gresty MA & Bronstein AM (2004). Perceptual and nystagmic thresholds of vestibular function in yaw. *J Vestib Res* **14**, 461–466.

Shimazu H & Precht W (1966). Inhibition of central vestibular neurons from the contralateral labyrinth and its mediating pathway. *J Neurophysiol* **29**, 467–492.

Smith CE & Goldberg JM (1986). A stochastic afterhyperpolarization model of repetitive activity in vestibular afferents. *Biol Cybern* **54**, 41–51.

Smith PF & Curthoys IS (1989). Mechanisms of recovery following unilateral labyrinthectomy: a review. *Brain Res Brain Res Rev* **14**, 155–180.

Smith PF, de Waele C, Vidal PP & Darlington CL (1991). Excitatory amino acid receptors in normal and abnormal vestibular function. *Mol Neurobiol* **5**, 369–387.

Snippe HP & Koenderink JJ (1992). Information in channel-coded systems: correlated receivers. *Biol Cybern* **67**, 183–190.

Stein RB, Gossen ER & Jones KE (2005). Neuronal variability: noise or part of the signal? *Nat Rev Neurosci* **6**, 389–397.

Straka H & Dieringer N (2004). Basic organization principles of the VOR: lessons from frogs. *Prog Neurobiol* **73**, 259–309.

Straka H, Vibert N, Vidal PP, Moore LE & Dutia MB (2005). Intrinsic membrane properties of vertebrate vestibular neurons: function, development and plasticity. *Prog Neurobiol* **76**, 349–392.

Sylvestre PA & Cullen KE (1999). Quantitative analysis of abducens neuron discharge dynamics during saccadic and slow eye movements. *J Neurophysiol* **82**, 2612–2632.

Tollin DJ, Koka K & Tsai JJ (2008). Interaural level difference discrimination thresholds for single neurons in the lateral superior olive. *J Neurosci* **28**, 4848–4860.

Valko Y, Lewis RF, Priesol AJ & Merfeld DM (2012). Vestibular labyrinth contributions to human whole-body motion discrimination. *J Neurosci* **32**, 13537–13542.

Wilson VJ, Yamagata Y, Yates BJ, Schor RH & Nonaka S (1990). Response of vestibular neurons to head rotations in vertical planes. III. Response of vestibulocollic neurons to vestibular and neck stimulation. *J Neurophysiol* **64**, 1695–1703.

Yu XJ, Dickman JD & Angelaki DE (2012). Detection thresholds of macaque otolith afferents. *J Neurosci* **32**, 8306–8316.

Zhou W, Tang BF, Newlands SD & King WM (2006). Responses of monkey vestibular-only neurons to translation and angular rotation. *J Neurophysiol* **96**, 2915–2930.

Additional information

Competing interests

None.

Author contributions

M.J. analysed and interpreted the data and drafted/revised the manuscript. D.E.M., A.D., and J.C. contributed to the analysis, interpreted the data, and drafted/revised the manuscript. S.G.S. carried out the recordings. K.E.C. conceived and supervised the project, interpreted the data and drafted/revised the manuscript and is responsible for the work. All the authors have read and approved the final version of this manuscript.